

# Three Projects in Astrophysical Magnetohydrodynamics

PI: David C. Collins (Florida State University)

## 1 Introduction

We are requesting  $5.8 \times 10^4$  SUs on Stampede 2 for the period beginning June 1, 2022. This allocation will support four projects involving astrophysical magnetic fields. The first project (*turbulence*) explores analytical formulae we have developed for isothermal turbulence, which is relevant for many astrophysical processes, among them the formation of stars. The second project (*cores*) simulates the formation of pre-stellar cores from low density interstellar clouds. The third project (*foregrounds*) examines the polarized signal produced by the interstellar medium, which is in the way of our understanding of the cosmic microwave background (CMB). The fourth project (*galaxies*) simulates entire galaxies, in order to understand the growth of the magnetic field. This research is supported by two NSF grants. The first two projects (*turbulence* and *cores*) are supported by NSF AST-1616026, and the third (*foregrounds*) is supported by NSF AST-2009870. We are hopeful that the *galaxies* project will be funded by a pending proposal.

These projects support three graduate students. Luz Jimenez Vela is working on the *cores* project; Branislav Rabatin is working on the *turbulence* and *foregrounds* projects; and Jacob Strack is working on the *galaxies* project.

Table ?? shows the cost for each project. Each of the four projects uses a slightly different physics package, which affects the cost of the simulation. In addition, two of the four projects employ adaptive mesh refinement (AMR), a technique that adaptively changes the resolution of the simulation. This also affects the cost of the simulation.

In Section 2 we motivate each project. In Section 3 we describe the computational tools to be used. In Section 4 we outline the simulations to be run and their projected cost.

## 2 Scientific Background

Here we will introduce the physical motivation for the projects, and describe the simulations to be performed. Detailed accounting of the performance and simulation structure can be found in Section 4.

### 2.1 Background: Turbulent Energy

Here we provide the background for the *turbulence* project (Section 2.1.1) and briefly motivate the simulations to support this study (Section 2.1.2). Details of the simulation cost can be found in Section 4.1.

#### 2.1.1 Motivation

The interstellar medium (ISM) is the gas between stars in the galaxy. It cools very effectively, so can be treated as isothermal [Krumholz star formation book](#). The ISM is also turbulent, with supersonic shocks driven by supernovae causing supersonic turbulence throughout the interstellar medium. This turbulence impacts the formation of stars (see Section 2.2) and causes a polarized screen that is blocking our view of the light from the big bang (see Section 2.4), among many other effects ([Elmegreen & Scalo 2004](#)). It is also interesting in its own right.

Supersonic turbulence is compressible, and the distribution of density fluctuations is described by a log normal, i.e. the log of density is distributed as a gaussian. The distribution of velocity is roughly Maxwellian, i.e. each of the components is a gaussian, and added in quadrature the distribution is Maxwellian. We have recently found analytic distributions for the internal energy and kinetic energy, as well as their joint

Table 1: STUFF

suite	$\sigma_v$	$\Delta x$	fv	$N_Z$	T	Delta T	$N_Z N_U$	$SU_{zu}$	su
turb	0.5	1/1024		$1.1 \times 10^9$	2.0	$7.0 \times 10^{-6}$	$3.0 \times 10^{14}$	$2.0 \times 10^{-11}$	$6.1 \times 10^3$
turb	1.0	1/1024		$1.1 \times 10^9$	1.0	$5.0 \times 10^{-6}$	$2.0 \times 10^{14}$	$2.0 \times 10^{-11}$	$4.0 \times 10^3$
turb	2.0	1/1024		$1.1 \times 10^9$	0.5	$4.0 \times 10^{-6}$	$1.5 \times 10^{14}$	$2.0 \times 10^{-11}$	$3.0 \times 10^3$
turb	4.0	1/1024		$1.1 \times 10^9$	0.3	$2.0 \times 10^{-6}$	$1.3 \times 10^{14}$	$2.0 \times 10^{-11}$	$2.5 \times 10^3$
turb	7.0	1/1024		$1.1 \times 10^9$	0.1	$1.0 \times 10^{-6}$	$1.2 \times 10^{14}$	$2.0 \times 10^{-11}$	$2.3 \times 10^3$
								SU	$1.8 \times 10^4$
								Disk	$5.6 \times 10^3$
suite	$\ell$	$\Delta x$	fv	$N_Z$	T	Delta T	$N_Z N_U$	$SU_{zu}$	su
cores	0	1.0 pc	1.00	$1.1 \times 10^9$	1 Myr	$3.0 \times 10^{-3}$ Myr	$3.1 \times 10^{11}$	$6.3 \times 10^{-11}$	$2.0 \times 10^1$
cores	1	0.5 pc	0.46	$4.0 \times 10^9$	1 Myr	$2.0 \times 10^{-3}$ Myr	$2.3 \times 10^{12}$	$6.3 \times 10^{-11}$	$1.4 \times 10^2$
cores	2	0.2 pc	0.08	$5.7 \times 10^9$	1 Myr	$9.0 \times 10^{-4}$ Myr	$6.6 \times 10^{12}$	$6.3 \times 10^{-11}$	$4.1 \times 10^2$
cores	3	0.1 pc	0.01	$7.0 \times 10^9$	1 Myr	$4.0 \times 10^{-4}$ Myr	$1.6 \times 10^{13}$	$6.3 \times 10^{-11}$	$1.0 \times 10^3$
cores	4	0.1 pc	0.00	$8.0 \times 10^9$	1 Myr	$2.0 \times 10^{-4}$ Myr	$3.7 \times 10^{13}$	$6.3 \times 10^{-11}$	$2.3 \times 10^3$
								per sim	$3.9 \times 10^3$
								SU	$1.2 \times 10^4$
								Disk	$1.6 \times 10^5$
suite	$M_{s,a}$	$\Delta x$	fv	$N_Z$	T	Delta T	$N_Z N_U$	$SU_{zu}$	su
CMB	1,1	1/1024	1.00	$1.1 \times 10^9$	3	$4.0 \times 10^{-5}$	$7.4 \times 10^{13}$	$6.2 \times 10^{-11}$	$4.6 \times 10^3$
CMB	1,5	1/1024	1.00	$1.1 \times 10^9$	3	$1.0 \times 10^{-5}$	$2.2 \times 10^{14}$	$6.2 \times 10^{-11}$	$1.4 \times 10^4$
CMB	5,1	1/1024	1.00	$1.1 \times 10^9$	0.6	$1.0 \times 10^{-5}$	$4.5 \times 10^{13}$	$6.2 \times 10^{-11}$	$2.8 \times 10^3$
CMB	5,5	1/1024	1.00	$1.1 \times 10^9$	0.6	$9.0 \times 10^{-6}$	$7.4 \times 10^{13}$	$6.2 \times 10^{-11}$	$4.6 \times 10^3$
								SU	$2.6 \times 10^4$
								Disk	$1.7 \times 10^4$
suite	$\ell$	$\Delta x$	fv	$N_Z$	T	Delta T	$N_Z N_U$	$SU_{zu}$	su
galaxy	0	$1.3 \times 10^6$ pc	$1.0 \times 10^0$	$1.7 \times 10^7$	1 Gyr	$4.0 \times 10^{-4}$ Gyr	$4.8 \times 10^{10}$	$3.0 \times 10^{-10}$	$1.4 \times 10^1$
galaxy	1	$2.6 \times 10^3$ pc	$1.0 \times 10^0$	$1.3 \times 10^8$	1 Gyr	$2.0 \times 10^{-4}$ Gyr	$7.6 \times 10^{11}$	$3.0 \times 10^{-10}$	$2.3 \times 10^2$
galaxy	2	$1.3 \times 10^3$ pc	$1.2 \times 10^{-1}$	$1.3 \times 10^8$	1 Gyr	$9.0 \times 10^{-5}$ Gyr	$1.5 \times 10^{12}$	$3.0 \times 10^{-10}$	$4.5 \times 10^2$
galaxy	3	$6.4 \times 10^2$ pc	$2.9 \times 10^{-2}$	$2.5 \times 10^8$	1 Gyr	$4.0 \times 10^{-5}$ Gyr	$5.7 \times 10^{12}$	$3.0 \times 10^{-10}$	$1.7 \times 10^3$
galaxy	4	$3.2 \times 10^2$ pc	$4.2 \times 10^{-3}$	$2.9 \times 10^8$	1 Gyr	$2.0 \times 10^{-5}$ Gyr	$1.3 \times 10^{13}$	$3.0 \times 10^{-10}$	$3.9 \times 10^3$
galaxy	6	$8.0 \times 10^1$ pc	$3.9 \times 10^{-4}$	$1.7 \times 10^8$	1 Gyr	$6.0 \times 10^{-6}$ Gyr	$3.1 \times 10^{13}$	$3.0 \times 10^{-10}$	$9.4 \times 10^3$
galaxy	9	$1.0 \times 10^1$ pc	$3.9 \times 10^{-5}$	$8.8 \times 10^7$	1 Gyr	$7.0 \times 10^{-7}$ Gyr	$1.3 \times 10^{14}$	$3.0 \times 10^{-10}$	$3.9 \times 10^4$
								per sim	$5.4 \times 10^4$
								SU	$1.1 \times 10^5$
								Disk	$1.1 \times 10^4$
								SU	$1.6 \times 10^5$
								Disk	$1.9 \times 10^5$

Table 2: Summary of simulation projects. The total node hours and disk usage are described in Section 4. The physics packages used in each project and adaptive mesh refinement (AMR) structure are described in Section 2

Name	Node Hours	Disk	Physics	AMR
Turbulence	1.8E+04	5.6E+03	Hydro + Driving	None
Cores	1.2E+04	1.6E+05	MHD + Gravity + Particles	4 levels, all space
CMB	2.6E+04	1.7E+04	MHD + Driving	None
Galaxies	1.1E+04	1.1E+04	MHD + Gravity + Star Formation	8 level nest
	6.6E+04	1.9E+05		

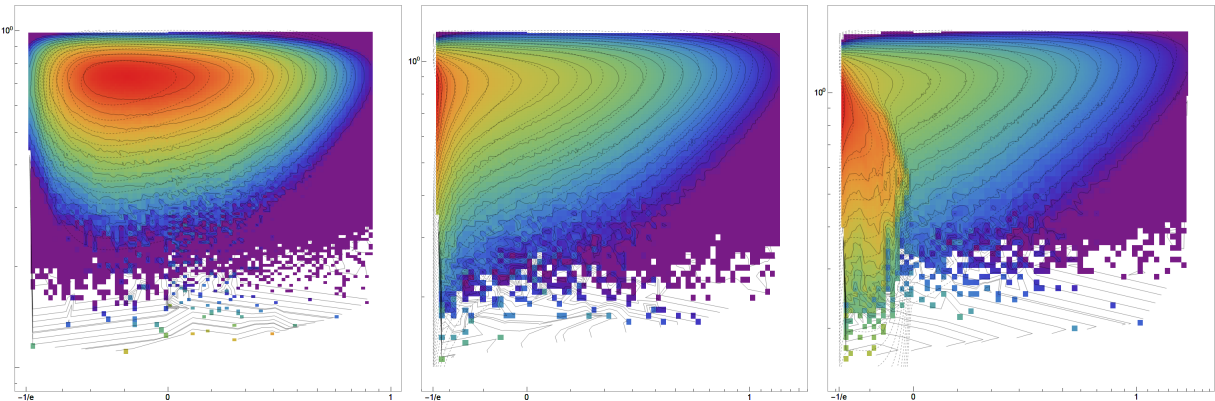


Figure 1: The joint distribution between thermal energy,  $E_T$ , and kinetic energy  $E_K$ . Color shows the PDF computed from low resolution simulations, and ranges between 0 (purple) and 1 (red). The thermal energy develops a low  $E_T$  wall as well as a high  $E_T$  wing as the Mach number increases. We will improve the noise and accuracy of these fits.

distribution. These energy distributions will be useful in future studies of turbulence in the ISM. We have verified these formulae with lower resolution simulations, with excellent but low-resolution agreement. Now we wish to verify the formulae with higher resolution simulations, and to explore if the small deviations from lognormal density and Maxwellian velocity that were seen in our preliminary runs are numerical, or something more interesting such as non-local transfer in the turbulent cascade.

Our analytic formulae predict, and the simulations reproduce, interesting changes in internal energy as the Mach,  $\mathcal{M}_S$ , number is increased. The Mach number,  $\mathcal{M}_S$ , is the r.m.s velocity relative to the speed of sound, and it dictates how compressible the flow is. We find that as  $\mathcal{M}_S$  is increases, a step forms at  $E_T = 0$ , which is reproduced by simulations.

We will perform a series of simulations increasing the r.m.s.

### 2.1.2 Simulations

Our simulations will begin with uniform density, and [magic paddles](#)

We will perform  $1024^3$  simulations because it should be a lot better

## 2.2 Background: Star Formation

Repeat the new things with higher resolution. Skip the chemistry discussion?

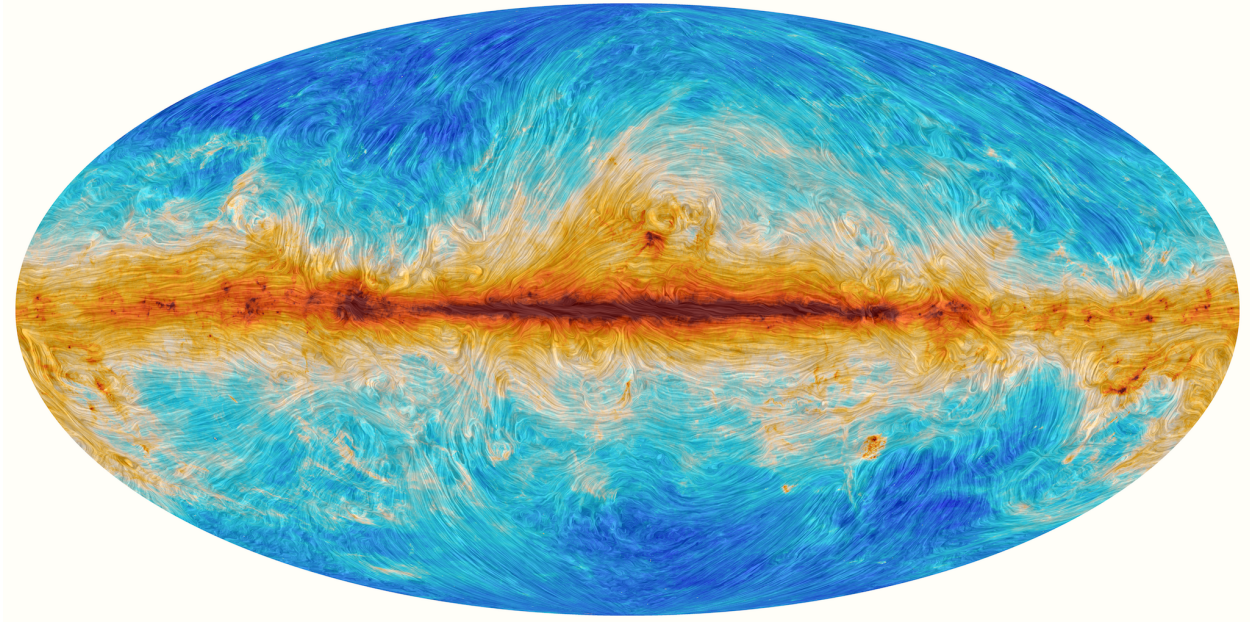


Figure 2: The large scale magnetic field of the galaxy as seen by the Planck satellite. The color field shows dust emission at 353GHz. The image is smeared along the direction of the magnetic field. ([Planck Collaboration et al. 2015](#))

### 2.3 Background: Galaxies

The *galaxies* project will simulate magnetic field generation in Milky Way sized galaxies. It is well known that the Milky Way has a large scale magnetic field of roughly  $\sim 6\mu\text{G}$ . For reference, 1G is about the strength of a refrigerator magnet. The Galactic magnetic field can be seen in Figure 2, which shows dust emission at 353 GHz. The map is smoothed in the direction of the magnetic field, showing large scale looping structures and small scale turbulent structures.

The origin of this magnetic field is an open question. There are presently two known *dynamos*, that is mechanisms to amplify magnetic fields. They differ in two ways; the length scales over which they act, and the time scales. The fast dynamo converts turbulent kinetic energy to magnetic energy at small scales, and produces disordered fields quickly. The slow dynamo produces large scale fields slowly, with large scale convective motions. The magnetic field in the Milky Way, as well as other similar galaxies, shows large scale order, but based on observations of galaxies, must have been built up quickly.

The magnetic field in the Galaxy is largely in one direction, loosely following the spiral arms. On the way to producing a large scale magnetic field, both mechanism produce a substantial amount of field in all directions. Thus to have a field of mostly one sign, the other sign must be expelled from the galaxy. Thus the buoyancy of the gas as it leaves the face of the disk is important in setting the rate of growth of the mean field. Like many problems in physics, the answer depends sensitively on boundary conditions, which in this case are poorly conscribed.

The circum-galactic medium (CGM) is the gas that's outside the galaxy, but still bound to it. It is extremely hot (millions of Kelvin) and extremely low density ( $0.1 \text{ cm}^{-3}$ ) and thus unfortunately difficult to constrain. The purpose of this project is to examine the growth of magnetic fields in Milky Way sized galaxies. Specifically, to examine the impact of the circum-galactic medium (CGM) properties on the dynamo. We expect that an ordered field within the disk requires a buoyant CGM, that is gas that is expelled from the

galaxy by supernovae continues to rise, rather than falling back down immediately. “

## 2.4 Background: Foregrounds

The cosmic microwave background (CMB) is the remnant radiation leftover from the Big Bang. It is extremely uniform on the sky, a perfect black body with a temperature of 2.7K. Its study, through satellites such as Planck, closed many open questions about the nature of the universe, such as its energy content and eventual fate. But it still has open questions.

When the universe was very young, it was very small, and also very hot. So hot that there were no atoms, only bare protons and electrons (and the occasional alpha particle.) Sound waves, triggered by the beginning event, locally compress and expand the gas, causing very small temperature fluctuations. As the universe expands, it cools. About 400,000 years after the beginning of time, the universe had cooled enough for the electrons and protons to meet and combine, rather than just scattering off one another. In a very short period of time, the universe all became neutral, and photons could travel great distances instead of bouncing off a nearby electron.

The fluctuations in the temperature are small, about a millionth of a Kelvin, but have allowed us to measure many factors of the universe. Chief among them are the curvature, mass density (both dark matter and luminous mass) and dark energy density. It has helped prove the acceleration of the expansion of the Universe. The CMB has helped answer many questions about the Universe.

Yet there are several questions that have not yet been answered, such as, why is it a single temperature? The universe is very large, and the CMB photons have traveled a great distance. So great, that the distance light has traveled during the age of the universe, when viewed at the distance of the CMB, is only the size of the full moon. So why is the same temperature everywhere? One possible answer is an extremely rapid *inflation* of the universe, where the universe expands from the size of a proton to the size of the solar system within the first  $10^{-16}$ . Such a violent event would leave a sea of gravitational waves. These gravitational waves, being quadrupolar in nature, imprint a polarization on the CMB. To detecting this polarization is to witness the violent birth of the Universe.

Unfortunately (and also fortunately, but for different reasons) the Galaxy we live in is filled with dust. This dust, which includes iron and magnesium, lines up perpendicular to the magnetic field in the galaxy, not unlike iron filings around a bar magnet. These dust grains radiate polarized thermal radiation in the microwave and infrared. This polarized signal is much brighter than the polarization in the CMB, so must be removed. In order to remove it, we must understand the statistical properties of the interstellar medium (ISM).

The Planck satellite [ref](#) measured the polarized sky, and the result can be seen in Figure [PLANCK](#). Statistically, the polarization is described best by the quantities  $E$  and  $B$ . The  $E$  mode is the amplitude in polarization that is either parallel to or perpendicular to filamentary structures, while  $B$  describes polarization at oblique angles. It is found that both structures are distributed over all scales in a power-law fashion, with  $E \propto k^{-2.35}$ , where  $k$  is wavenumber on the sky.  $B$  has a similar exponent but half the amplitude.

Our group has had success in reproducing similar behavior in a few settings. In [Stalpes](#) we demonstrated that MHD turbulence can reproduce similar exponents, with the value of the exponent and amplitude depending on velocity and magnetic field strength in the turbulence. In [?](#), we developed a model of the ISM polarization based on magnetized filaments.

In the proposed simulations, we will combine these two approaches. We will perform a series of driven turbulent boxes, as described in [REF](#), but this time with magnetic fields. We will then use the filament finding tool [DISPERSE](#) [disperse](#)

The study of the ISM is very rich. We are embarking of two lines of study. The first uses the galaxies of the *galaxies* project. We will use the galaxies of that suite of study to constrain the available polarization signals

## 3 Computational Method

We will use Enzo.

SF: Enzo + Particles

Galaxies: Chemistry and SF and all that stuff

CMB: Enzo + MHD

Turb: Enzo + PPM

## 4 Simulation Plan

Here we will outline the simulations to be performed for each of the projects.

The total cost for one simulation is determined by multiplying the cost for a single zone-update by the number of zones and the number of updates. Thus,  $SU = SU_{zu}ZU$ , where  $SU$  is the total cost,  $SU_{zu}$  is cost in  $SU$ -per-zone-update,  $Z$  is the number of zones, and  $U$  is the number of updates.  $SU_{zu}$  is determined by the total speed of all of the physics packages employed for each time step, and is different for each simulation suite. The choice of physics package was motivated in Section 2, and the measurement of  $SU_{zu}$  is presented in the Scaling and Performance document. The estimate of the number of zones,  $Z$ , comes from a combination of the simulation domain and the expected number of zones for each level of the simulation. The number of updates,  $U$ , is found as  $U = T/\Delta t$ , where the total simulation time is  $T$  and the size of the timestep is  $\Delta t$ .  $T$  is determined by the physics problem. For all of our simulations, the size of the time step  $\Delta t$  is determined by a standard Courant condition, that is a wave cannot cross half of one zone in a timestep. That is,

$$\Delta t = \eta \frac{\Delta x}{v_{\text{signal}}} \quad (1)$$

, and  $\eta < 0.5$ . We determine  $v_{\text{signal}}$ , the fastest signal speed, from preliminary studies, use Equation 1 to determine the number of steps on each level. For each suite of simulations, we determine the performance  $SU_{zu}$  from preliminary studies that closely mirror the simulation structure and physics packages.

### 4.1 Simulations: Turbulent Energy

### 4.2 Simulations: Star Formation

Big tracer runs.

### 4.3 Simulations: Galaxies

Really, this is "get something off the ground."

### 4.4 Simulations: Foregrounds

Big magnetic simulations.

## 5 Access to Other Computational Resources

**Local Computing Environment** The astrophysics group at Florida State University has a small cluster with 300 cores. This machine is useful for testing and debugging, but not large enough for the proposed

Table 3: STUFF

suite	$\sigma_v$	$\Delta x$	fv	$N_Z$	T	Delta T	$N_Z N_U$	$SU_{zu}$	su
turb	0.5	1/1024		$1.1 \times 10^9$	2.0	$7.0 \times 10^{-6}$	$3.0 \times 10^{14}$	$2.0 \times 10^{-11}$	$6.1 \times 10^3$
turb	1.0	1/1024		$1.1 \times 10^9$	1.0	$5.0 \times 10^{-6}$	$2.0 \times 10^{14}$	$2.0 \times 10^{-11}$	$4.0 \times 10^3$
turb	2.0	1/1024		$1.1 \times 10^9$	0.5	$4.0 \times 10^{-6}$	$1.5 \times 10^{14}$	$2.0 \times 10^{-11}$	$3.0 \times 10^3$
turb	4.0	1/1024		$1.1 \times 10^9$	0.3	$2.0 \times 10^{-6}$	$1.3 \times 10^{14}$	$2.0 \times 10^{-11}$	$2.5 \times 10^3$
turb	7.0	1/1024		$1.1 \times 10^9$	0.1	$1.0 \times 10^{-6}$	$1.2 \times 10^{14}$	$2.0 \times 10^{-11}$	$2.3 \times 10^3$
								SU	$1.8 \times 10^4$
								Disk	$5.6 \times 10^3$
suite	$\ell$	$\Delta x$	fv	$N_Z$	T	Delta T	$N_Z N_U$	$SU_{zu}$	su
cores	0	1.0 pc	1.00	$1.1 \times 10^9$	1 Myr	$3.0 \times 10^{-3}$ Myr	$3.1 \times 10^{11}$	$6.3 \times 10^{-11}$	$2.0 \times 10^1$
cores	1	0.5 pc	0.46	$4.0 \times 10^9$	1 Myr	$2.0 \times 10^{-3}$ Myr	$2.3 \times 10^{12}$	$6.3 \times 10^{-11}$	$1.4 \times 10^2$
cores	2	0.2 pc	0.08	$5.7 \times 10^9$	1 Myr	$9.0 \times 10^{-4}$ Myr	$6.6 \times 10^{12}$	$6.3 \times 10^{-11}$	$4.1 \times 10^2$
cores	3	0.1 pc	0.01	$7.0 \times 10^9$	1 Myr	$4.0 \times 10^{-4}$ Myr	$1.6 \times 10^{13}$	$6.3 \times 10^{-11}$	$1.0 \times 10^3$
cores	4	0.1 pc	0.00	$8.0 \times 10^9$	1 Myr	$2.0 \times 10^{-4}$ Myr	$3.7 \times 10^{13}$	$6.3 \times 10^{-11}$	$2.3 \times 10^3$
								per sim	$3.9 \times 10^3$
								SU	$1.2 \times 10^4$
								Disk	$1.6 \times 10^5$
suite	$M_{s,a}$	$\Delta x$	fv	$N_Z$	T	Delta T	$N_Z N_U$	$SU_{zu}$	su
CMB	1,1	1/1024	1.00	$1.1 \times 10^9$	3	$4.0 \times 10^{-5}$	$7.4 \times 10^{13}$	$6.2 \times 10^{-11}$	$4.6 \times 10^3$
CMB	1,5	1/1024	1.00	$1.1 \times 10^9$	3	$1.0 \times 10^{-5}$	$2.2 \times 10^{14}$	$6.2 \times 10^{-11}$	$1.4 \times 10^4$
CMB	5,1	1/1024	1.00	$1.1 \times 10^9$	0.6	$1.0 \times 10^{-5}$	$4.5 \times 10^{13}$	$6.2 \times 10^{-11}$	$2.8 \times 10^3$
CMB	5,5	1/1024	1.00	$1.1 \times 10^9$	0.6	$9.0 \times 10^{-6}$	$7.4 \times 10^{13}$	$6.2 \times 10^{-11}$	$4.6 \times 10^3$
								SU	$2.6 \times 10^4$
								Disk	$1.7 \times 10^4$
suite	$\ell$	$\Delta x$	fv	$N_Z$	T	Delta T	$N_Z N_U$	$SU_{zu}$	su
galaxy	0	$1.3 \times 10^6$ pc	$1.0 \times 10^0$	$1.7 \times 10^7$	1 Gyr	$4.0 \times 10^{-4}$ Gyr	$4.8 \times 10^{10}$	$3.0 \times 10^{-10}$	$1.4 \times 10^1$
galaxy	1	$2.6 \times 10^3$ pc	$1.0 \times 10^0$	$1.3 \times 10^8$	1 Gyr	$2.0 \times 10^{-4}$ Gyr	$7.6 \times 10^{11}$	$3.0 \times 10^{-10}$	$2.3 \times 10^2$
galaxy	2	$1.3 \times 10^3$ pc	$1.2 \times 10^{-1}$	$1.3 \times 10^8$	1 Gyr	$9.0 \times 10^{-5}$ Gyr	$1.5 \times 10^{12}$	$3.0 \times 10^{-10}$	$4.5 \times 10^2$
galaxy	3	$6.4 \times 10^2$ pc	$2.9 \times 10^{-2}$	$2.5 \times 10^8$	1 Gyr	$4.0 \times 10^{-5}$ Gyr	$5.7 \times 10^{12}$	$3.0 \times 10^{-10}$	$1.7 \times 10^3$
galaxy	4	$3.2 \times 10^2$ pc	$4.2 \times 10^{-3}$	$2.9 \times 10^8$	1 Gyr	$2.0 \times 10^{-5}$ Gyr	$1.3 \times 10^{13}$	$3.0 \times 10^{-10}$	$3.9 \times 10^3$
galaxy	6	$8.0 \times 10^1$ pc	$3.9 \times 10^{-4}$	$1.7 \times 10^8$	1 Gyr	$6.0 \times 10^{-6}$ Gyr	$3.1 \times 10^{13}$	$3.0 \times 10^{-10}$	$9.4 \times 10^3$
galaxy	9	$1.0 \times 10^1$ pc	$3.9 \times 10^{-5}$	$8.8 \times 10^7$	1 Gyr	$7.0 \times 10^{-7}$ Gyr	$1.3 \times 10^{14}$	$3.0 \times 10^{-10}$	$3.9 \times 10^4$
								per sim	$5.4 \times 10^4$
								SU	$1.1 \times 10^5$
								Disk	$1.1 \times 10^4$
								SU	$1.6 \times 10^5$
								Disk	$1.9 \times 10^5$

simulations. Florida State University also maintains a research cluster, but it is also insufficient for this research.

**Other supercomputing resources.** The PI of the current proposal does not presently have access to other supercomputing resources.

## 6 Personnel

The PI of this project is Dr. David C. Collins, an Associate Professor in the Florida State University Department of Physics. Dr. Collins has more than fifteen years of experience working using high performance computing platforms for research in computational astrophysics. He is also a lead developer of the code Enzo, which has a long history of simulation success.

Three PhD students will be working on the projects. Luz Jimenez Vela will be responsible for the *cores* project. Branislav Rabatin is responsible for both the *turbulence* and *foregrounds* projects. Jacob Strack is responsible for the *galaxies* project.

## References

Elmegreen, B. G. & Scalo, J. 2004, ARA&A, 42, 211

Planck Collaboration, Ade, P. A. R., Aghanim, N., Alina, D., Alves, M. I. R., Armitage-Caplan, C., Arnaud, M., Arzoumanian, D., Ashdown, M., Atrio-Barandela, F., Aumont, J., Baccigalupi, C., Banday, A. J., Barreiro, R. B., Battaner, E., Benabed, K., Benoit-Lévy, A., Bernard, J. P., Bersanelli, M., Bielewicz, P., Bock, J. J., Bond, J. R., Borrill, J., Bouchet, F. R., Boulanger, F., Bracco, A., Burigana, C., Butler, R. C., Cardoso, J. F., Catalano, A., Chamballu, A., Chary, R. R., Chiang, H. C., Christensen, P. R., Colombi, S., Colombo, L. P. L., Combet, C., Couchot, F., Coulais, A., Crill, B. P., Curto, A., Cuttaia, F., Danese, L., Davies, R. D., Davis, R. J., de Bernardis, P., de Gouveia Dal Pino, E. M., de Rosa, A., de Zotti, G., Delabrouille, J., Désert, F. X., Dickinson, C., Diego, J. M., Donzelli, S., Doré, O., Douspis, M., Dunkley, J., Dupac, X., Efstathiou, G., Enßlin, T. A., Eriksen, H. K., Falgarone, E., Ferrière, K., Finelli, F., Forni, O., Frailis, M., Fraisse, A. A., Franceschi, E., Galeotta, S., Ganga, K., Ghosh, T., Giard, M., Giraud-Héraud, Y., González-Nuevo, J., Górski, K. M., Gregorio, A., Gruppuso, A., Guillet, V., Hansen, F. K., Harrison, D. L., Helou, G., Hernández-Monteagudo, C., Hildebrandt, S. R., Hivon, E., Hobson, M., Holmes, W. A., Hornstrup, A., Huffenberger, K. M., Jaffe, A. H., Jaffe, T. R., Jones, W. C., Juvela, M., Keihänen, E., Keskitalo, R., Kisner, T. S., Kneissl, R., Knoche, J., Kunz, M., Kurki-Suonio, H., Lagache, G., Lähteenmäki, A., Lamarre, J. M., Lasenby, A., Lawrence, C. R., Leahy, J. P., Leonardi, R., Levrier, F., Liguori, M., Lilje, P. B., Linden-Vørnle, M., López-Caniego, M., Lubin, P. M., Macías-Pérez, J. F., Maffei, B., Magalhães, A. M., Maino, D., Mandolesi, N., Maris, M., Marshall, D. J., Martin, P. G., Martínez-González, E., Masi, S., Matarrese, S., Mazzotta, P., Melchiorri, A., Mendes, L., Mennella, A., Migliaccio, M., Miville-Deschénes, M. A., Moneti, A., Montier, L., Morgante, G., Mortlock, D., Munshi, D., Murphy, J. A., Naselsky, P., Nati, F., Natoli, P., Netterfield, C. B., Noviello, F., Novikov, D., Novikov, I., Oxborrow, C. A., Pagano, L., Pajot, F., Paladini, R., Paoletti, D., Pasian, F., Pearson, T. J., Perdereau, O., Perotto, L., Perrotta, F., Piacentini, F., Piat, M., Pietrobon, D., Plaszczynski, S., Poidevin, F., Pointecouteau, E., Polenta, G., Popa, L., Pratt, G. W., Prunet, S., Puget, J. L., Rachen, J. P., Reach, W. T., Rebolo, R., Reinecke, M., Remazeilles, M., Renault, C., Ricciardi, S., Riller, T., Ristorcelli, I., Rocha, G., Rosset, C., Roudier, G., Rubiño-Martín, J. A., Rusholme, B., Sandri, M., Savini, G., Scott, D., Spencer, L. D., Stolyarov, V., Stompor, R., Sudiwala, R., Sutton, D., Suur-Uski, A. S., Sygnet, J. F., Tauber, J. A., Terenzi, L., Toffolatti, L., Tomasi, M., Tristram, M., Tucci, M., Umana, G., Valenziano, L.,

Valiviita, J., Van Tent, B., Vielva, P., Villa, F., Wade, L. A., Wandelt, B. D., Zacchei, A., & Zonca, A. 2015, A&A, 576, A104